Russian Journal of Organic Chemistry, Vol. 40, No. 6, 2004, pp. 837–846. Translated from Zhurnal Organicheskoi Khimii, Vol. 40, No. 6, 2004, pp. 876–885.

Dynamic Intramolecular Rearrangements with Proton Transfer in Methanimine Oxide

R. M. Aminova[1] and E. A. Ermakova[2]

[1] *Kazan State University, ul. Kremlevskaya 18, Kazan, 420008 Tatarstan, Russia*
e-mail: aminov@ksu.ru

[2] *Kazan Institute of Biochemistry and Biophysics, Kazan Research Center, Russian Academy of Sciences, Kazan, Tatarstan, Russia*

Received April 11, 2003

Abstract—The structures of possible intermediates and transition states on the potential energy surface for the isomerization of methanimine oxide into formamide were determined by UHF/6-311G(3*d*) quantum-chemical calculations. Two possible reaction channels were revealed. The same processes were studied by the direct molecular mechanics method which also revealed two reaction channels. The time range of the examined dynamic processes was estimated at 90–300 fs.

Extensive experimental studies in the field of optical spectroscopy at pico- and femtosecond levels [1–3] of two- [4–8] and polyatomic molecules [9–12] stimulate development of theoretical approaches to interpretation of the results of such experiments. Therefore, application of such theoretical methods for studying reaction mechanisms as quantum chemistry and nonempirical molecular dynamics becomes actual.

The goal of the present work was to examine the possibility of joint application of both traditional quantum-chemical methods [13, 14] and nonempirical molecular dynamics (NMD) to analysis of the mechanism of intramolecular rearrangement of methanimine oxide into formamide, which involves proton transfer.

In the recent years, *ab initio* molecular dynamics [15–17], specifically the direct dynamics (DD) method [18–29, 41, 42], attracted increasing attention. These methods imply calculation of the interaction potentials directly while building up the trajectory for movement of a molecular system at a semiempirical or nonempirical level. This makes it possible to simulate the dynamic behavior of a system where bond cleavage or closure occurs and hence to obtain information on the time span of processes under study. Taking the above into account, DD may be a good auxiliary method which probably may compete with standard quantum-chemical procedures for localizing transition states and calculating potential energy surfaces. Here, we report on our first experience in using DD for studying isomerization processes, and the DD calculations are auxiliary.

It is known that derivatives of azomethine oxides (which are generically called *nitrones*) $CHR^1{=}N(O)R^2$ (R^1 = Ph, R^2 = $C_6H_4NO_2$) are photochemically active [30]; therefore, they may be promising subjects for optical studies in the pico- and femtosecond ranges. Irradiation of azomethine oxides gives rise to isomeric oxaziridines which are capable of undergoing thermal or photochemical rearrangement into amides [31–36]. From this viewpoint, studies of isomerization processes in such systems by quantum-chemical methods and molecular dynamics attract considerable interest.

In the present work we examined intramolecular rearrangements of methanimine oxide $CH_2{=}N(O)H$ which can be regarded as a model of more complex photochemically active derivatives like *C*-4-nitrophenyl-*N*-phenylnitrone 4-$NO_2C_6H_4C(H){=}N(O)Ph$. Isomerization processes are characterized by many degrees of freedom, and their interpretation is generally difficult even for a molecular system in the ground state. The availability of experimental data and relative simplicity of the system make it a convenient model for studying more complex molecules.

In keeping with the commonly accepted views, azomethine oxides are usually represented as three canonical structures **I**–**III**.

1070-4280/04/4006-0837

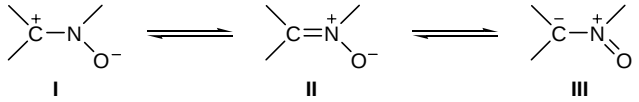

I II III

From the viewpoint of reactivity, structure **I** ("extended carbonyl") is the most significant, for nitrones undergo electrophilic attack at the oxygen atom, and nucleophilic attack, at the carbon atom. The isomerization scheme is shown below:

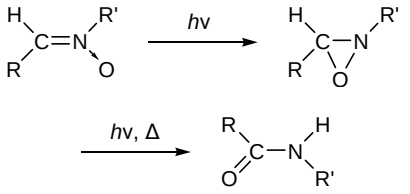

The calculations of the energies and electronic and geometric parameters of the reactant (R), product (P), intermediates (Int), and transition states (TS) were performed by the PM3 semiempirical method and *ab initio*, in terms of the unrestricted Hartree–Fock–Roothaan procedure with the 3-21G, 6-31G, and 6-311G(3*d*) basis sets. Complete analysis of vibrational frequencies was performed for stationary points, and the internal reaction coordinate (IRC) [38] was calculated to make sure that the transition states found correspond to the processes under study. The calculations were performed using GAMESS [37] and GAUSSIAN 94 software packages [38].

Table 1. Total and relative energies of the initial reactant, final product, intermediates, and transition states calculated by the UHF/6-311G(3*d*) with account taken of zero-point vibration energy

Species	E_{tot}, a.u.	E_{rel}, kcal/mol
R (reactant)	–168.813072	0
TS1	–168.712037	63.4
Int1 (oxaziridine)	–168.813613	–0.34
TS2	–168.803617	5.93
Int2	–168.836368	–14.62
TS3	–168.786250	16.83
Int3	–168.906931	–58.90
TS4	–168.840174	–17.01
TS5	–168.793900	12.03
P (product)	–168.935708	–76.9

The molecular dynamics calculations (DD) were performed using HyperChem Demo version [39]. Here, the dynamics of nuclear motion is described by classical Newton equations [40], but the interaction potentials are calculated at a semiempirical or nonempirical level at every time step. The MD calculations were performed in two modes. According to the first of these, the interaction potentials were calculated by the PM3 semiempirical method, and in the second case, nonempirical method with the 6-31G* basis set was applied. A typical PM3 trajectory had a lifetime of 2 to 5 ps, and 6-31G* trajectory, 0.5 to 1 ps; the time step was set at 0.2 fs. Using quantum-chemical methods, we localized stationary points on the unexcited potential energy surface and calculated the energies (Table 1) and geometric parameters (Table 2) of the reactant (R), three-membered oxaziridine intermediate (Int1), and final product P (Fig. 1).

The quantum-chemical calculations showed that the trajectory from R to Int1 includes one transition state TS1 (Fig. 2). As compared to the initial geometry, the N–O bond in TS1 extends to 1.33 Å, the ONC angle decreases to 92.4°, and the N–H[6] and N–O bonds deviate from coplanarity. As a result, the N(O)H group appears turned apart in such a way that the lone electron pair (LEP) on the nitrogen atom becomes coplanar to the CH_2 fragment. The energy of activation with respect to the ground state of R is fairly high, 64.69 kcal/mol. Internal reaction coordinate calculations starting from the TS1 geometry gave the initial reactant structure while descending in one direction and oxaziridine structure while descending in the other direction. The energy of oxaziridine is less than that of R by only 0.34 kcal/mol.

The trajectory from oxaziridine to the final product, formamide, is considerably more intricate. According to the quantum-chemical calculations, it includes two intermediates Int2 and Int3 and, correspondingly, three transition states, TS2, TS3, and TS4 (Figs. 1, 2). In the initial part of that trajectory, the N–O bond extends relative to the equilibrium value in oxaziridine (1.43 Å). Opening of the three-membered ring begins with elongation of the N–O bond [6-311G(3*d*) calculations give the initial N–O bond length 1.44 Å] and gradual increase of the NCO bond angle [equilibrium value 62.5°; 6-311G(3*d*)]. Analysis of the potential energy surface (PES) for a series of N–O bond lengths with optimization of all other parameters showed formation of a diradical singlet N–O structure when the N–O bond length reaches 1.64 Å [3-21G, 6-311(3*d*)]: the spin densities on the nitrogen and oxygen atoms

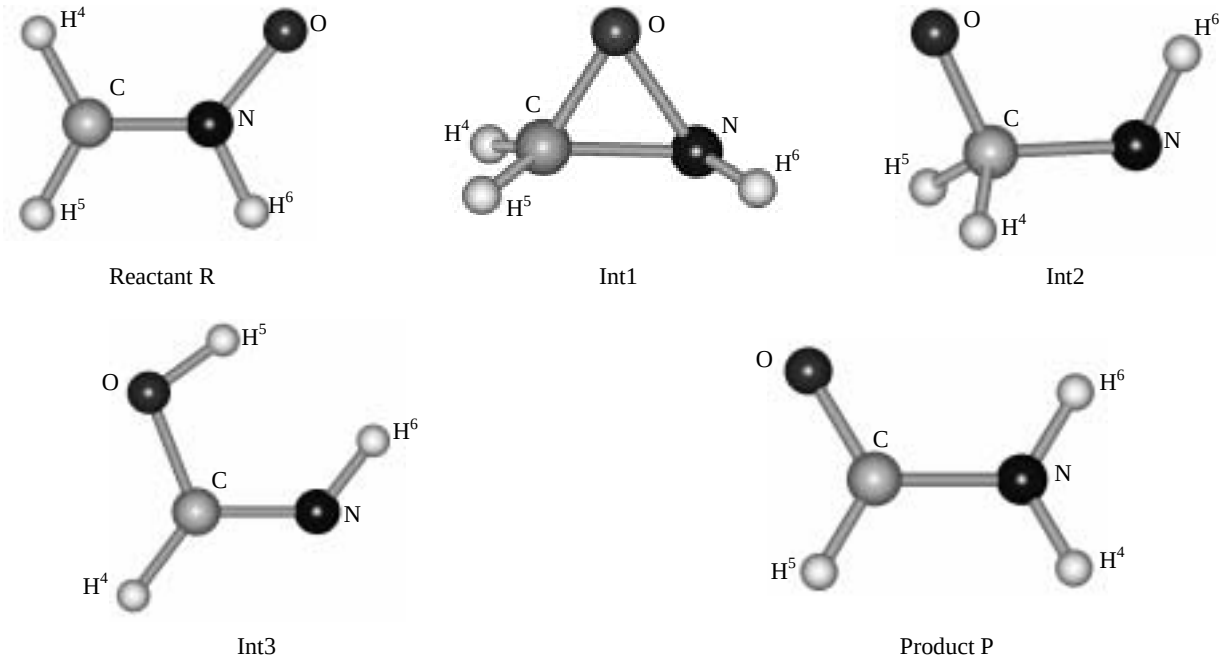

Fig. 1. Structures of the reactant, intermediates, and final product, calculated by the UHF 6-311G(3*d*) method.

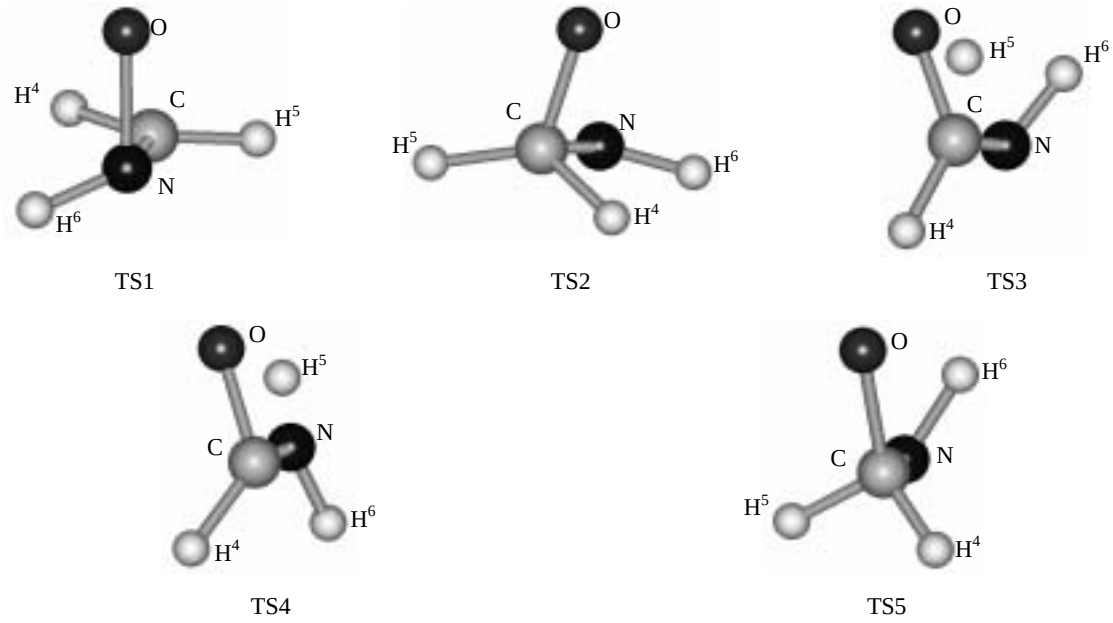

Fig. 2. Structures of the transition states, calculated by the UHF 6-311G(3*d*) method; first reaction channel: TS1, TS2, TS3, and TS4; second reaction channel: TS1, TS2, and TS5.

acquire non-zero values, 0.61 and –0.56, respectively. Simultaneously, the N–H^6 bond turns to increase the dihedral angle H^6NCH^4, while the dihedral angle $OCNH^6$ decreases. As a result, an equilibrium open-chain configuration, intermediate Int2, is formed. The dihedral angle H^6NCO therein is close to zero (the N–H^6 and C–O bonds are eclipsed) (Fig. 2, TS2). Opening of the three-membered ring via cleavage of the N–O bond occurs in such a way that the C–O bond appears *trans* relative to the nitrogen LEP. This is consistent with the known fact [43] that lone electron pair has a larger volume than electron pair involved in a single bond; therefore, *trans* configuration ensures minimal stereoelectronic repulsion.

Table 2. Geometric parameters (interatomic distances, Å, and angles, deg) of the reactant (R), product (P), transition states (TS), and intermediates (Int), calculated by the UHF/6-311G(3*d*) method[a]

Parameter	R	TS1	TS2	TS3	TS4	Int1	Int2	Int3	Int4	P
C–N	1.27	1.32	1.42	1.33	1.28	1.42	1.41	1.43	1.24	1.36
C–O	2.26	1.92	1.36	1.35	1.26	1.25	1.37	1.37	1.33	1.18
N–O	1.25	1.33	1.66	2.38	2.06	2.37	1.44	2.39	2.33	2.25
$O\cdots H^4$	2.55	2.13	2.07	1.32	1.31	2.02	2.08	1.99	0.94	2.50
$C\cdots H^4$	1.07	1.07	1.08	1.25	1.56	1.08	1.08	1.09	1.89	2.01
$C\cdots H^5$	1.07	1.08	1.08	1.08	1.08	1.23	1.08	1.09	1.07	1.09
$N\cdots H^5$	2.01	2.09	2.11	2.06	2.12	1.48	2.12	2.06	2.01	2.04
$N\cdots H^4$	2.01	2.08	2.15	2.14	1.32	2.10	2.15	2.06	2.46	0.99
CNO	128.4	92.4	51.8	27.98	35.3	25.7	57.4	30.6	26.4	25.5
OCN	25.6	44.0	73.2	124.5	108.5	124.9	62.5	117.3	129.2	125.0
CON	26.0	–	55.0	27.5	36.2	29.4	60.2	32.1	24.4	29.5
CNH^6	116.1	125.2	107.8	108.8	125.5	106.3	108.9	107.7	113.0	118.6
NCH^4	118.8	120.0	118.6	112.3	54.3	113.4	119.6	108.8	101.4	26.2
NCH^5	118.5	120.9	114.5	117.2	128.2	67.5	116.3	108.8	120.5	112.8
H^4CH^5	122.7	118.9	113.6	110.4	177.5	106.2	115.6	106.8	138.1	138.1
H^4CO	93.2	86.1	115.6	60.9	54.2	119.6	116.0	107.4	27.8	99.5
H^5CO	144.1	138.7	115.6	115.9	123.3	108.9	116.4	107.4	110.3	122.2
ONH^6	115.5	119.0	99.6	80.9	160.9	80.82	104.6	77.1	86.7	142.2
$ONCH^4$	0.0	–44.7	–110.5	–69.1	0.0	–	–105.8	122.0	0.0	14.5
$ONCH^5$	180.0	129.9	111.0	161.7	–180.0	–	107.6	–122.0	–180.0	–178
H^4CNH^6	180.0	83.8	–22.2	–63.9	–179.9	–171.8	–10.3	122.1	–0.03	–147
H^5CNH^6	0.0	–101.5	–160.7	166.9	0.04	89.6	–157.0	–122.0	–180.0	20.4
$OCNH^6$	–	128.5	88.3	5.2	–179.9	–8.4	95.5	–0.03	–0.02	–161

[a] TS1 is the transition state between methanimine oxide and oxaziridine; TS2 is the transition state between oxaziridine and intermediate Int2 (acyclic structure with eclipsed C–O and N–H^6 bonds); TS3 is the transition state between Int2 and Int3 [C(OH)H=NH]; TS4 is the transition state between Int3 and formamide (first reaction channel); and TS5 is the transition state between Int2 and formamide (second reaction channel).

Comparison of the energies and geometric parameters of transition state TS2 calculated with different basis sets showed that inclusion of *d* orbitals [6-311(3*d*)] appreciably reduces the activation barrier separating oxaziridine and Int2 (TS2): its height is equal to 5.93 kcal/mol with respect to the initial reactant and 6.27 kcal/mol with respect to oxaziridine.

We revealed two reaction channel starting from open-chain structure Int2. One of these includes formation of intermediate Int3 and hence two transition states (TS3 between Int2 and Int3 and TS4 between Int2 and formamide; Fig. 3). The formation of Int3 is accompanied by abstraction of H^4 (Fig. 2, TS3) and its subsequent addition to the oxygen atom. The distance between H^4 and C^1 in TS3 is 1.25 Å, and the distance between the abstracted H^4 atom and oxygen is 1.32 Å. The activation barrier for the transformation of Int2 into Int3 (Table 1) is 31.45 kcal/mol. According to the IRC calculations, descend in one direction leads to open-chain structure Int 2, and in the other direction, to Int3. This process is exothermic, the energy of the reaction at that stage is 44.28 kcal/mol. The C–O–N

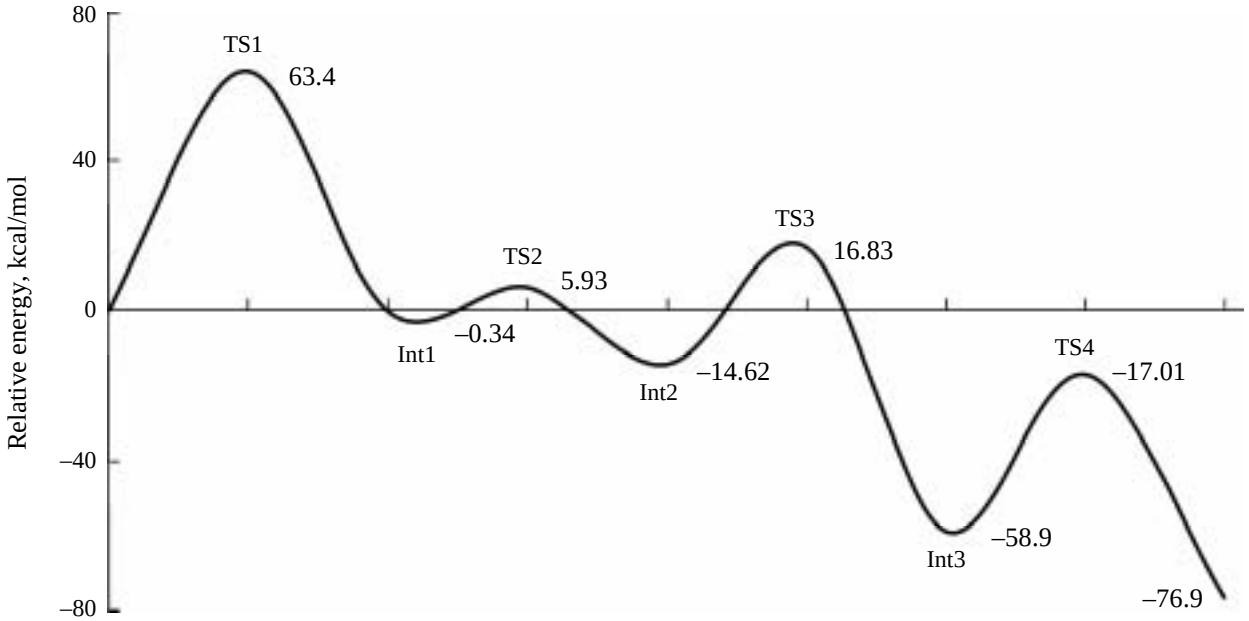

Fig. 3. Energy diagram of the reaction path for the rearrangement of methanimine oxide into formamide (first channel).

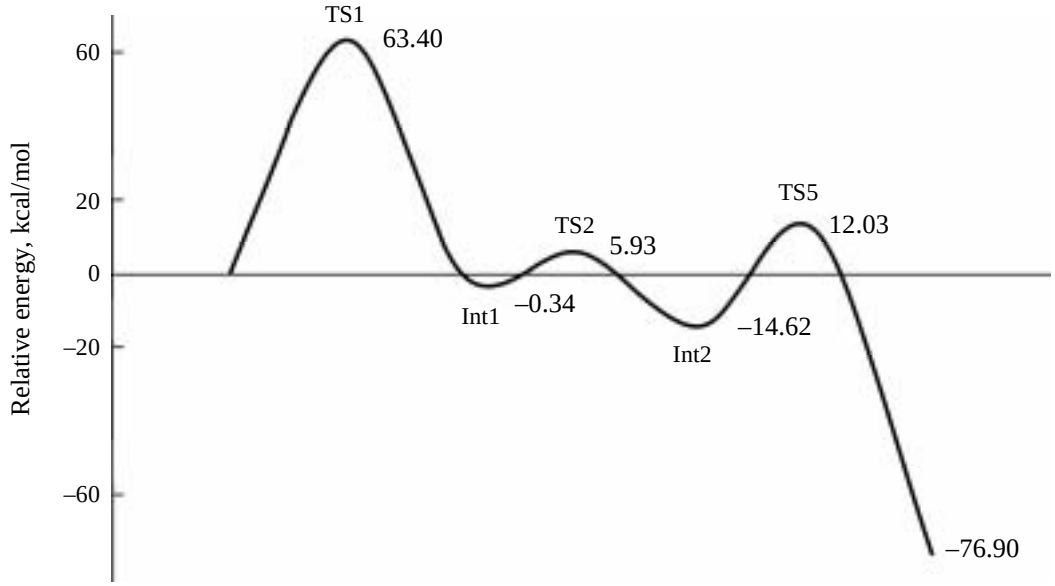

Fig. 4. Energy diagram of the reaction path for the rearrangement of methanimine oxide into formamide (second channel).

group and N–H bond in Int3 are arranged *cis* with respect to each other, so that the C–O–H group is located *trans* relative to LEP on the nitrogen atom. As noted above, *trans* arrangement relative to the nitrogen LEP is characterized by weaker stereoelectronic repulsion, as compared to the *cis* arrangement. The trajectory from Int3 to product P passes through transition state TS4 where H^4 is removed from the oxygen atom (the distances from H^4 to the oxygen, nitrogen, and carbon atoms are 1.31, 1.32, and 1.56 Å, respectively).

The calculations also revealed another reaction channel. It coincides with the first one in going from methanimine oxide (R) to oxaziridine (Int1) and from Int1 to open-chain structure Int2. Further on, the second channel directly leads to formamide through transition state TS5 (Fig. 4). Here, the H^5 atom adds to the nitrogen, while H^6 remains in the *cis* position with respect to the oxygen atom. The second channel is more favorable from the viewpoint of energy than the first channel involving formation of intermediate Int3 with O–N bond. The energy difference is 4.8 kcal/mol.

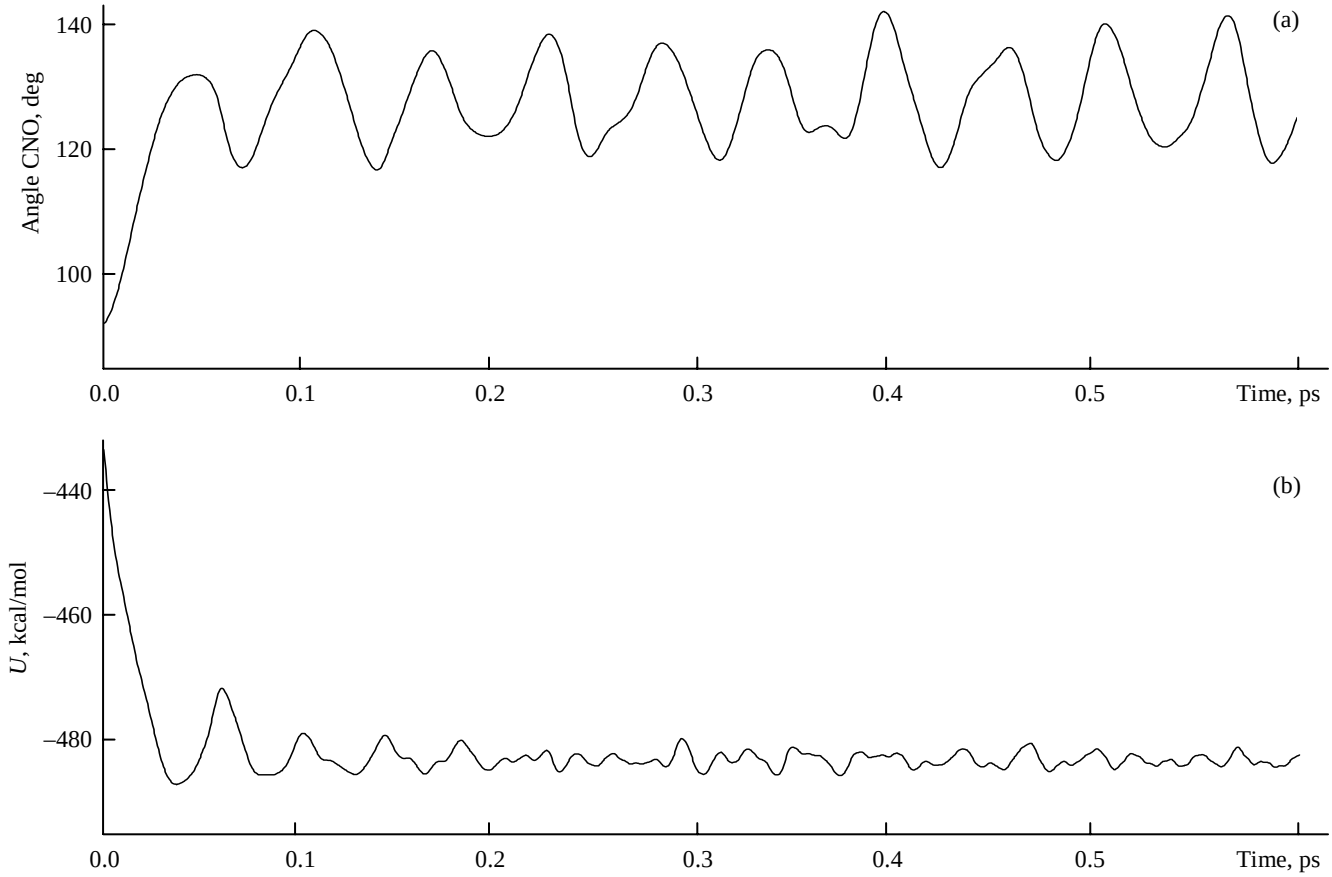

Fig. 5. Variation of the (a) CNO bond angle (deg) and (b) potential energy (kcal/mol) along the trajectory from transition state TS1 to reactant R.

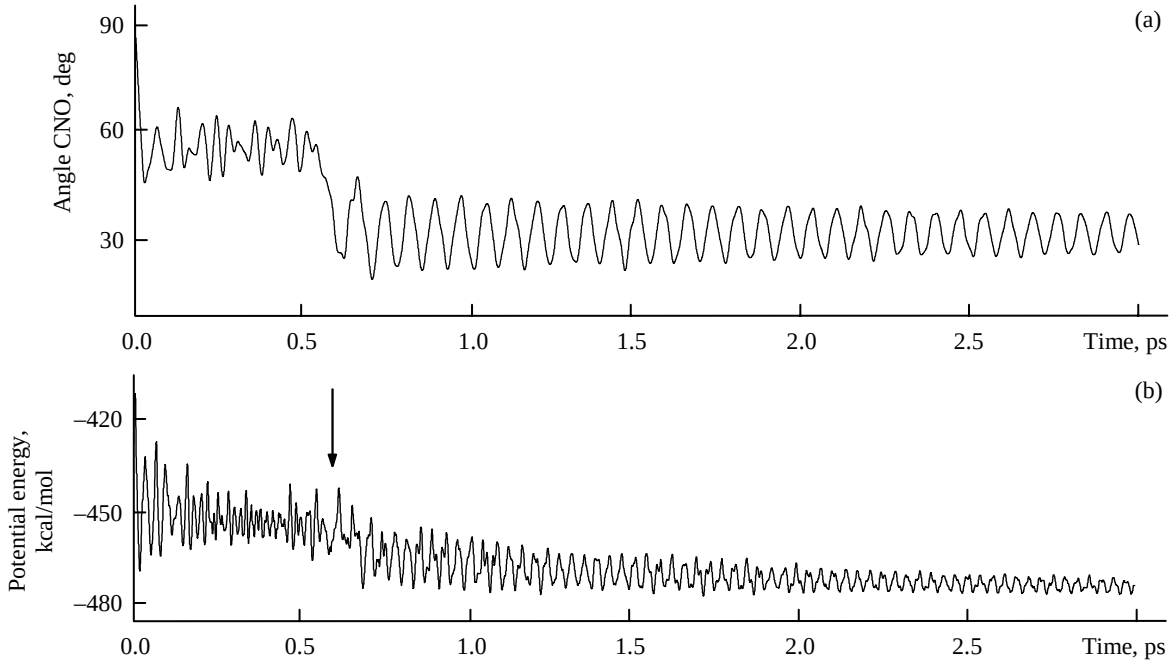

Fig. 6. Evolution of the system from transition state TS1 through intermediate Int1 and transition state TS2 toward intermediate Int2. Variation of the (a) CNO bond angle (deg) and (b) potential energy (kcal/mol) along the trajectory from transition state TS1 to intermediate Int2.

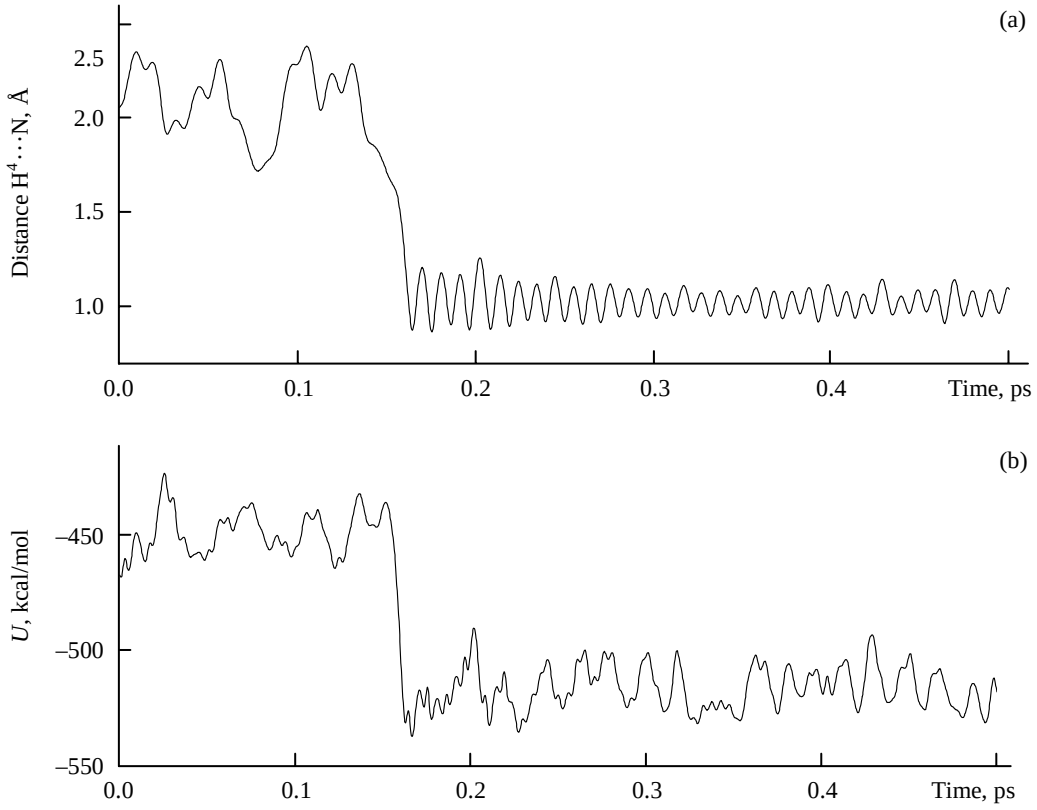

Fig. 7. Dynamics of the molecule in going from intermediate Int2 through transition state TS5 to the product. Variation of the (a) $H^4\cdots N$ distance (Å) and (b) potential energy (kcal/mol) with time.

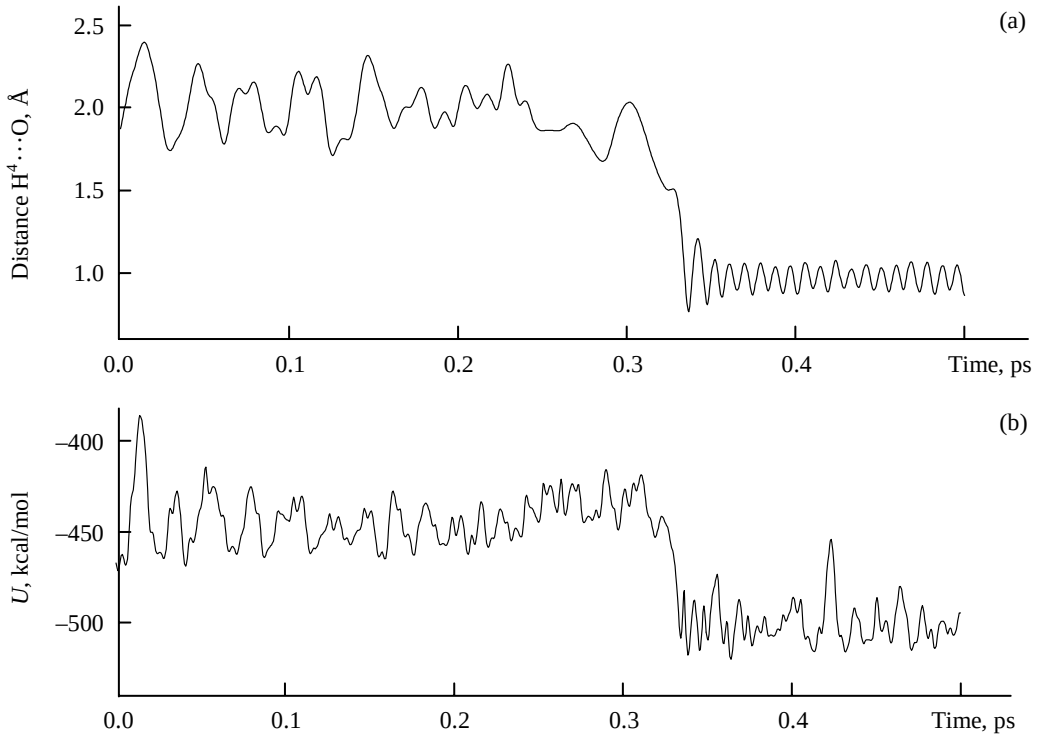

Fig. 8. Variation of the (a) $H^4\cdots O$ distance (Å) and (b) total energy of the system (kcal/mol) in going from intermediate Int2 to Int3.

While performing molecular dynamics calculations, it should be recognized that chemical reaction is a very rare case. In other words, only one of numerous collisions is accompanied by such energy redistribution in a molecule which allows it to overcome the energy barrier. In order to reveal this spontaneous chemical reaction, a very long trajectory should be built up for a system consisting of a huge number of molecules. Insofar as such problem cannot be solved at present, we tried to simulate the process by reacting a single molecule and starting the calculations from the first transition state (TS1).

To a first approximation, both semiempirical (Figs. 5–8) and nonempirical calculations gave qualitatively similar patterns; therefore, we will not discuss the details arising from the use of different basis sets. Depending on the initial rate distribution, the system can move from TS1 either backward (toward the initial reactant) or forward (toward the product). While moving forward, the potential energy (Fig. 5a) and the bond angle CNO (Fig. 5b) change with time (the CNO angle varies from 90 to ~125°). These data are fully consistent with the calculated geometric parameters of TS1 and R. No specific points on that trajectory were found, and the system quickly returns to the initial state (R). Here, the DD calculations are very similar to IRC; however, the former provide some information on the time scale of the process. It is seen that the trajectory from TS1 to R has a lifetime of about 10 fs.

According to the DD calculations, the system can also move from TS1 to P via two different paths. Depending on the kinetic energy of the system and its initial distribution over degrees of freedom, the system can pass in succession through Int1, TS2, Int2, and TS5 to P or, if the total energy is insufficient or the energy distribution over degrees of freedom is unfavorable, it may stay for a fairly long period (up to several picoseconds) at intermediate states Int1 or Int2; in these cases, an additional kinetic energy redistribution is necessary to force the system to leave the intermediate state.

Figures 6–8 show trajectories from the initial reactant to the product. The initial sharp drop in the potential energy (Fig. 6b) corresponds to the transition from TS1 to Int1 where the molecule stays for about 500 fs. Next follows slight increase in the potential energy (indicated with an arrow in Fig. 6b); it corresponds to passing through the second transition state (TS2) to local minimum Int2 and is accompanied by sharp variation of the CNO bond angle (Fig. 6a).

The existence of a small potential barrier between oxaziridine and open-chain structure Int2 is very consistent with the results of quantum-chemical calculations. In fact, a potential barrier of 6.24 kcal/mol was found between Int1 and Int2 (Table 1). If the energy distribution in the system is favorable, the reaction is completed by transfer of H^4 or H^5 to the nitrogen atom (yielding the final product) in ~100–300 fs. If the energy distribution over degrees of freedom is unfavorable, the system may stay at Int2 for a fairly long time (the maximal observation period was 5 ps). In going from Int2 to formamide (Fig. 7), the potential energy maximum (approximately in 150 fs from the trajectory start) corresponds to transition state TS5 (Fig. 7b) where the distance between the H^4 and nitrogen atoms is about 1.4 Å (Fig. 7a). After that point, the potential energy sharply decreases. This reaction path coincides with that found by the quantum-chemical calculations (see above, path *2*).

Aida *et al*. [18] presumed that, generally speaking, the IRC path can differ from the path for a system characterized by a non-zero velocity along the reaction coordinate at a finite temperature. When a system possesses a definite total energy, it may go from one state to another by-passing transition state or take a way which is less favorable from the viewpoint of activation barriers calculated by quantum-chemical methods. Nevertheless, the existence of another reaction channel which was revealed by quantum-chemical calculations (Fig. 2) is also confirmed by the molecular dynamics study. Before Int2, the critical points at that trajectory are the same as those described above for the first channel. If the system stays at Int2 for a long time, transfer of H^4 to the oxygen atom is possible, and it leads to structure Int3 through transition state TS3. The formation of intermediate structure Int3, where the H^4 atom is attached to oxygen, is accompanied by rotation of the O–H^4 bond about the O–C axis to give the corresponding transition state TS4, and only then the system goes to the product.

It is seen that the transformation of Int2 into Int3 (Fig. 8) is characterized by a fairly high activation barrier. This does not contradict the results of quantum-chemical calculations. According to the data in Table 1, the potential barrier to the transition Int2 → Int3 is 31.45 kcal/mol. Also, a high potential barrier (41.89 kcal/mol) separates Int3 from the product. This path corresponds to the first channel described above. Complete analysis of the energy profile for the rearrangement of methanimine oxide

into formamide along two channels leads us to conclude that the second (shorter) channel is preferred.

Finally, it should be emphasized that the results of the quantum-chemical study are well consistent with those obtained by the direct dynamics study; in addition, the two methods supplement each other. They revealed two reaction channels on the ground-state potential energy surface for the rearrangement of methanimine oxide. The preferred channel starts from the initial reactant and leads to three-membered intermediate through transition state TS1, acyclic intermediate Int2 through transition state TS2, and the final product through transition state TS5. The H^4 or H^5 proton is directly transferred to the nitrogen atom. Opening of the three-membered intermediate (oxaziridine Int1) at the N–O bond gives rise to a singlet diradical structure which is converted into Int2 with eclipsed C–O and N–H bonds. The second channel coincides with the first one at the path from R to Int2. However, the subsequent trajectory leading to the final product includes two transition states TS3 and TS4 and intermediate Int3.

The application of femtosecond spectroscopic methods in studies of photoinduced molecular rearrangement processes inevitably requires detailed analysis of excited states of molecular systems. This topic will be the subject of our subsequent publication.

The authors greatly acknowledge S.A. Moiseev, R.M. Minyaev, and A.G. Shamova for very fruitful discussion of the results and helpful suggestions.

This study was performed under financial support by the Russian Foundation for Basic Research (project nos. 01-03-32730, 03-03-96214r2003tatarstan, and 03-04-96276r2003tatarstan) and by the Tatarstan Republic Foundation "Research and Experimental Developments" [project no. 06-6.3-154/2002F(06)].

REFERENCES

1. Zewail, A.H., *Femtochemistry: Ultrafast Dynamics of the Chemical Bond*. Singapore: World Scientific, 1994, vols. 1, 2.
2. *Femtosecond Chemistry*, Manz, J. and Woste, L., Eds., Weinheim: VCH, 1995.
3. Zhong, D., Diau, E.W.-G., Bernhardt, T.M., De Feyter, S., Roberts, J.D., and Zewail, A.H., *Chem. Phys. Lett*., 1998, vol. 298, p. 129.
4. Herek, J.L., Materny, A., and Zewail, A.H., *Chem. Phys. Lett*., 1994, vol. 228, p. 15.
5. Dietz, H. and Engel, V., *Chem. Phys. Lett*., 1996, vol. 255, p. 258.
6. Andersson, L.M., Karlsson, H.O., Goscinski, O., Berg, L.-E., Beutter, M., and Hansson, T., *Chem. Phys*., 1999, vol. 241, p. 43.
7. Sarkisov, O.M., Tovbin, D.V., Lozovoy, V.V., Gostev, F.E., Titov, A.A., Antipin, S.A., and Umanskiy, S.Ya., *Chem. Phys. Lett*., 1999, vol. 303, p. 458.
8. Lozovoy, V.V., Antipin, S.A., Gostev, F.E., Titov, A.A., Tovbin, D.V., Sarkisov, O.M., Vetchinkin, A.S., and Umanskiy, S.Ya., *Chem. Phys. Lett*., 1998, vol. 284, p. 221.
9. Zhang, J.Z., Schwartz, B.J., King, J.C., and Harris, C.B., *J. Am. Chem. Soc*., 1992, vol. 114, p. 10921.
10. Felker, P.M., Lambert, Wm.R., and Zewail, A.H., *J. Chem. Phys*., 1982, vol. 77, p. 1603.
11. Antipin, S.A., Petrukhin, A.N., Gostev, F.E., Marevtsev, V.S., Titov, A.A., Barachevsky, V.A., Strokach, Yu.P., and Sarkisov, O.M., *Chem. Phys. Lett*., 2000, vol. 331, p. 378.
12. Dzhemesyuk, O.A., Antipin, S.A., Gostev, F.E., Fedorovich, I.B., Sarkisov, O.M., and Ostrovskii, M.A., *Dokl. Ross. Akad. Nauk*, 2002, vol. 382, p. 699.
13. Minkin, V.I., Simkin, B.Ya., and Minyaev, R.M., *Teoriya stroeniya molekul* (Theory of Molecular Structure), Rostov-on-Don: Feniks, 1997, p. 558.
14. Minyaev, R.M., *Usp. Khim*., 1994, vol. 63, p. 939.
15. Car, R. and Parinello, M., *Phys. Rev. Lett*., 1985, vol. 55, p. 2471.
16. Marx, D. and Huter, J., *Ab initio Molecular Dynamics: Theory and Implementation in Modern Methods and Algorithms of Quantum Chemistry*, Grotendorst, J., Ed., Julich, 2000, p. 149.
17. Tuckerman, E., Ungar, P.J., von Rosenvinge, T., and Klein, M.L., *J. Phys. Chem*., 1996, vol. 100, p. 12788.
18. Aida, M., Yamataka, H., and Dupuis, M., *Theor. Chem. Acc*., 1999, vol. 102, p. 262.
19. Skokov, S. and Wheeler, R.A., *J. Phys. Chem. A*, 2000, vol. 104, p. 6314.
20. Truhlar, D.G., *The Reaction Path in Chemistry: Current Approaches and Perspectives*, Heidrich, D., Ed., Dordrecht: Kluwer, 1995, p. 229.
21. Steckler, R., Thurman, G.M., Watts, J.D., and Bartlett, R.J., *J. Chem. Phys*., 1997, vol. 106, p. 3926.
22. Wei, D. and Salahub, D.R., *J. Chem. Phys*., 1997, vol. 106, p. 6086.
23. Ishikawa, Y. and Binning, Jr.R.C., *Chem. Phys. Lett*., 2002, vol. 358, p. 509.
24. Doubleday, C., Bolton, K., and Hase, W.L., *J. Phys. Chem. A*, 1998, vol. 102, p. 3648.
25. Li, G. and Hase, W.L., *J. Am. Chem. Soc*., 1999, vol. 121, p. 7124.
26. Zhang, X., Ding, Y., Li, Z., Huang, X., and Sun, Ch., *Chem. Phys. Lett*., 2000, vol. 330, p. 577.

27. Li, Sh., Yu, X., Xu, Zh., Li, Z., and Sun, Ch., *J. Mol. Struct. (Theochem)*, 2001, vol. 540, p. 221.
28. Bolton, K., Hase, W.L., Schlegel, H.B., and Song, R., *Chem. Phys. Lett*., 1998, vol. 288, p. 621.
29. Peslherbe, G.H., Wang, H., and Hase, W.L., *J. Am. Chem. Soc*., 1996, vol. 118, p. 2257.
30. Splitter, J. and Calvin, M., *J. Org. Chem*., 1965, vol. 30, p. 3427.
31. Spence, G.G., Taylor, E., and Buchardt, O., *Chem. Rev*., 1970, vol. 70, p. 231.
32. Shinzawa, K. and Tanaka, I., *J. Phys. Chem*., 1964, vol. 68, p. 1205.
33. Koyano, K. and Tanaka, I., *J. Phys. Chem*., 1965, vol. 69, p. 2545.
34. Koyano, K., Suzuki, H., Mori, Y., and Tanaka, I., *Bull. Chem. Soc. Jpn*., 1970, vol. 43, p. 3582.
35. Krishan, K. and Singkh, Kh., *Izv. Akad. Nauk SSSR, Ser. Khim*., 1974, p. 1404.
36. Fukui, K., *Acc. Chem. Res*., 1981, vol. 14, p. 363.
37. Schmidt, M.W., Baldridge, K.K., Boatz, J.A., Elbert, S.T., Gordon, M.S., Jensen, J.H., Koseki, H., Matsunaga, N., Nguyen, K.A., Su, S.J., Windus, T.L., Dupuis, M., and Montgomery, A., *J. Comput. Chem*., 1993, vol. 14, p. 1347.
38. Frisch, M.J, Trucks, G.W., Schlegel, H.B., Gill, P.M.W., Johnson, B.G., Robb, M.A., Cheeseman, J.R., Keith, T., Petersson, G.A., Montgomery, J.A., Raghavachari, K., Al-Laham, M.A., Zakrzewski, V.G., Ortiz, J.V., Foresman, J.B., Cioslowski, J., Stefanov, B.B., Nanayakkara, A., Challacombe, M., Peng, C.Y., Ayala, P.Y., Chen, W., Wong, M.W., Andres, J.L., Replogle, E.S., Gomperts, R., Martin, R.L., Fox, D.J., Binkley, J.S., Defrees, D.J., Baker, J., Stewart, J.P., Head-Gordon, M., Gonzalez, C., and Pople, J.A., *Gaussian 94, Revision D*, Pittsburgh PA: Gaussian, 1995.
39. *HyperChem 5.0 for Windows*, Hypercube, 1994–1995.
40. Allen, M.P. and Tildesley, D.J., *Computer Simulation of Liquids*, Oxford: Clarendon, 1987, p. 385.
41. Doubleday, C., *Chem. Phys. Lett*., 1995, vol. 233, p. 509.
42. Doubleday, C., Bolton, K., Peslherbe, G.H., and Hase, W.L., *J. Am. Chem. Soc*., 1996, vol. 118, p. 9922.
43. Gillespie, R.J., *Molecular Geometry*, New York: Reinhold, 1972.